

## Resistivity and the Hall effect in polycrystalline Ni–Cu and Ta–Cu multi-layered thin films

G Reiss, K Kapfberger, G Meier, J Vancea and H Hoffmann

Institut für Angewandte Physik III, Universität Regensburg, Regensburg, Federal Republic of Germany

Received 17 May 1988, in final form 1 August 1988

**Abstract.** In the present paper the dependences of the resistivity  $\rho$  and the Hall voltage  $U_H$  of polycrystalline Ni–Cu and Ta–Cu multi-layered thin films on the layer thickness  $d_i$  are discussed. The thickness dependence of  $\rho$  and  $U_H$  can be well understood using a simple model in which the layers are considered as parallel resistors, whereby the resistivity of a single layer is enhanced via surface scattering described by the well known Fuchs–Namba size theory.

The Hall coefficients are independent of the layer thickness, although the measured Hall voltage varies with  $d_i$  owing to the enhancement of the individual layer resistivities. For very thin layers, i.e. if the layer thickness becomes smaller than the layer roughness, the experimental data on both  $\rho$  and  $U_H$  indicate a breakdown of the multi-layered structure to an island-like clustered film structure. For Ni–Cu a crossover from ferroparamagnetic to superparamagnetic behaviour was observed at this critical thickness.

### 1. The resistivity of multi-layered structures

The resistivity of multi-layered metal structures has been treated in [1–6]. These theories are in fact applications of the theory of Fuchs [7] who calculated the thickness-dependent resistivity of a single layer by solving the Boltzmann equation with respect to appropriate boundary conditions. Within this framework the influence of the surface is introduced using the ‘specularity parameter’  $p$  describing either specular ( $p$ ) or diffuse ( $1-p$ ) scattering of conduction electrons at surfaces and interfaces. Specular reflection of the conduction electrons means conservation of the momentum parallel to the surface or interface and therefore does not enhance the resistivity, whereas diffuse scattering is described by a constant probability for the electron to be scattered into all allowed  $k$ -states. This second mechanism leads to an increase in the resistivity of thin films compared with the corresponding value of the bulk material.

As demonstrated by recent experiments [8, 9] a continuous coverage of a single-layer metal film with another metal reduces the specularity parameter approximately to zero. In multi-layered films the layers therefore become decoupled and the resistivity of the films resulting from the theories mentioned above is

$$\rho = (d_a + d_b)\rho_a(d_a)\rho_b(d_b)/[d_a\rho_b(d_b) + d_b\rho_a(d_a)]. \quad (1)$$

Here  $d_a$ ,  $d_b$ ,  $\rho_a(d_a)$  and  $\rho_b(d_b)$  are the layer thicknesses and resistivities of metals a and b, respectively.

The thickness-dependent resistivities  $\rho_i(d_i)$  of ideal flat single layers of metal  $i$  are given by the usual single-layer Fuchs equation for  $p = 0$  [7, 10]:

$$\rho_i(d_i) = \rho_{\infty i} \left\{ 1 - \frac{3l_{\infty i}}{2d_i} \int_1^{\infty} (t^{-3} - t^{-5}) \left[ 1 - \exp\left(-\frac{d_i}{l_{\infty i}} t\right) \right] dt \right\}^{-1} \quad (2)$$

where  $\rho_{\infty i}$  is the corresponding bulk resistivity and  $l_{\infty i}$  is the background electronic mean free path (MFP).

In the case of rough films the surface roughness should be additionally introduced by averaging equation (2) over a film with fluctuating thickness  $d(x)$  using the well known model of Namba [11] (see also [12]):

$$\rho_i(d_i, l_i) = \langle \rho_i(d_i(x)) \rangle_{\text{film}} \quad (2a)$$

where  $\langle \dots \rangle$  denotes average and  $d_i$  is the mean layer thickness.

## 2. Hall effect in multi-layered systems

In [13] both the Hall voltage  $U_H$  and the Hall coefficient  $R_H$  for the normal Hall effect in multi-layered continuous films were derived:

$$U_H = [U_H^a \rho_b(d_b) d_a + U_H^b \rho_a(d_a) d_b] / [\rho_a(d_a) d_a + \rho_b(d_b) d_b] \quad (3)$$

$$R_H = (d_a + d_b) [R_H^a \rho_b^2(d_b) d_a + R_H^b \rho_a^2(d_a) d_b] / [\rho_b(d_b) d_a + \rho_a(d_a) d_b]^2. \quad (4)$$

Here  $U_H^i = I_i R_H^i B / d_i$  is the Hall voltage for metal  $i$  and  $I_i$  is the current flowing through metal  $i$ ;  $B$  is the applied magnetic field.

If the multi-layered structure is broken owing to island-like growth at extremely small layer thicknesses, the model in [14] for binary alloys seems to be more appropriate. Here the Hall voltage is given by

$$U_H = BI(r_a R_H^a + r_b R_H^b) \quad (5)$$

with

$$r_a = x^2(\sigma^2 - 1)/(x^2 - 1)\sigma^2 \quad (5a)$$

$$r_b = (x^2 - \sigma^2)/(x^2 - 1)\sigma^2 \quad (5b)$$

$$\sigma = (1 - x)(0.5 - c) + \sqrt{(1 - x)^2(0.5 - c)^2 + x} \quad (5c)$$

where  $x = \rho_b / \rho_a$  and  $c$  is the concentration of the  $a$  component.

For the Ni-Cu system the magnetisation of Ni produces an anomalous contribution to the Hall voltage. The dependence of  $U_H$  on  $B$  then is given by

$$U_H = I_{\text{Ni}} R_1^{\text{Ni}} M_{\text{Ni}}(B) + U_H^0 \quad (6)$$

with  $I_{\text{Ni}}$  the current flowing through the Ni component,  $R_1^{\text{Ni}}$  the anomalous Hall coefficient of Ni,  $M_{\text{Ni}}(B)$  the magnetisation of the Ni component and  $U_H^0$  the normal Hall voltage. For ferromagnetic behaviour and fields above the saturation field, equation (6) reduces to

$$U_H = I_{\text{Ni}} R_1^{\text{Ni}} M_s^{\text{Ni}} + U_H^0 \quad (7)$$

where  $M_s^{\text{Ni}}$  is the saturation magnetisation of Ni.

For island-like clustered films a crossover from ferromagnetism to superparamagnetism, i.e. the paramagnetism produced in this case by the small weakly interacting ferromagnetic Ni particles, can be expected [15]. Here, no saturation field can be defined. In terms of the well known Langevin function [16] the magnetisation will be given by

$$M_{\text{Ni}}(B) = N\mu[\coth(\mu B/k_{\text{B}}T) - k_{\text{B}}T/\mu B] \quad (8)$$

where  $\mu$  is the mean magnetic moment of a Ni cluster and  $N$  is the total number of clusters.

### 3. Film production and measurement technique

The multi-layered structures were prepared by DC magnetron sputtering from two sources onto Corning glass substrates. The base pressure was  $1 \times 10^{-7}$  mbar; the argon sputtering pressure of  $1 \times 10^{-3}$  mbar was held constant during the sputtering process.

The substrates could be positioned alternatively over each magnetron source by means of a rotating substrate holder. The thickness was monitored using a quartz oscillator (Balzers) with a relative accuracy of  $10^{-4}$ .

All the experiments described in this paper have been carried out at room temperature. The resistivity was measured by a conventional DC four-probe technique; a lock-in system was used for measuring the Hall voltage with AC (33 Hz) currents of 2.5 mA (Ta–Cu) and 10 mA (Ni–Cu) at a magnetic field of 4 T for the Ta–Cu films and fields up to 6 T for the Ni–Cu films. The absolute accuracy of the results obtained amounts to 5% for both the resistivity and the Hall voltage, mainly owing to absolute errors in thickness; the relative accuracy is 0.5% for the resistivity and 2% for the Hall voltage.

## 4. Results and discussion

### 4.1. The resistivity

The dependence of the resistivity on the layer thickness is shown in figure 1 in a  $\rho$  against  $1/d_i$  plot. The thicknesses  $d_i^j$  of the individual layers of material  $i$  ( $i = \text{Ni–Cu}$  or  $\text{Ta–Cu}$ ) were equal (i.e.  $d_1 = d_1^{\text{Ni}} = d_1^{\text{Cu}}$  and  $d_1 = d_1^{\text{Ta}} = d_1^{\text{Cu}}$ ); the total thickness was approximately 100 nm.

The resistivity increases smoothly with decreasing layer thickness down to  $d_1 = 1.6$  nm for Ta–Cu and to  $d_1 = 1$  nm for Ni–Cu. Below these critical values, the resistivity becomes essentially constant close to the measured value of the corresponding alloys (marked by arrows in figure 1). In figure 1 the full curves are the results of fitting the combined equations (1) and (2) to the measured values. The parameters evaluated from these calculations are listed in table 1.

The resistivity  $\rho_{\infty}$  for the bulk materials corresponds to fine-grained polycrystals. As shown in earlier publications [8, 9, 12], the main contribution to the resistivity in such materials is due to grain boundary scattering of the conduction electrons. Therefore the inner-crystalline MFP  $l_{\infty}$  is not as drastically reduced as the resistivity is enhanced. Within the accuracy of the fitting procedure (20% for the MFP) the background MFP  $l_{\infty}$  agrees with earlier measurements of the group in Regensburg [8, 9, 12].

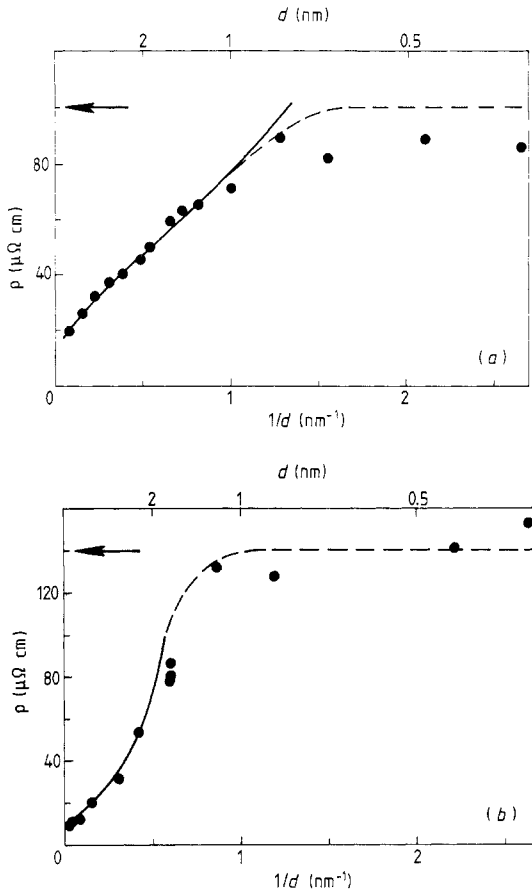


**Figure 1.** Resistivity  $\rho$  plotted against inverse layer thickness  $1/d$ , for (a) Ni-Cu and (b) Ta-Cu at  $T = 300$  K; ●, experimental results; —, theory (equations (1) and (2)); ←, alloy value; ---, guide for the eye.

The total roughness  $h$  resulting from the fitting calculations is approximately 1.4 nm for Ta-Cu and 1.0 nm for Ni-Cu (as listed in table 1); the relative error of the obtained values amounts to 20%. Owing to these small values of  $h$ , neither scanning nor transmission electron microscopy can be used to measure the roughness directly. Direct measurements of  $h$  by means of scanning tunnelling microscopy are in progress; the first

**Table 1.** Results for the parameters of the single-layer Fuchs-Namba model from the fitting calculation.

Structure	Layer	$\rho_\infty$ ( $\mu\Omega$ cm)	$l_\infty$ (nm)	$h$ (nm)	$p$
Ni-Cu	Ni	36.6	15	0.5	0
Ni-Cu	Cu	6.1	20	0.5	0
Ta-Cu	Ta	205	0.5	0.2	0
Ta-Cu	Cu	4.4	24	1.2	0

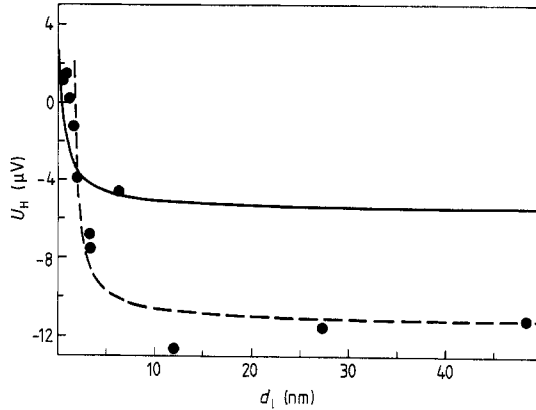


**Figure 2.** Hall voltage plotted against layer thickness for Ta–Cu ( $B = 4$  T;  $I = 2.5$  mA;  $T = 300$  K; film width, 0.2 cm): ●, experimental results; ---, model in [13]; —, model in [14].  $1 \mu\text{V}$  corresponds to a total Hall constant of  $1 \times 10^{-11} \text{ m}^3 \text{ C}^{-1}$ .

results, which will be presented elsewhere, show very flat film surfaces with a residual roughness of about 2 nm for both types of film, in good agreement with the fitting results. Owing to these values of the film roughnesses, the curves shown in figure 1 clearly have to be divided into two parts: layer thickness  $d_1$  greater than the film roughness  $h$ ; layer thickness  $d_1$  smaller than the film roughness  $h$ . For  $d_1 > h$  the model of parallel switched double layers, together with the Fuchs–Namba term for the individual single-layer resistivity, fits the experimental data well, as shown in figure 1 and as discussed above. For  $d_1 < h$  the films become discontinuous, i.e. the structure changes from multi-layered to island-like or clustered two-component films. This change in structure is accompanied by a saturation of the resistivity to a value very close to that of Ni–Cu and Ta–Cu alloys, respectively. The measured values for the corresponding alloys are given in figure 1.

The model of parallel switched double layers fits the dependence of the resistivity on the layer thickness of course only for continuous films, i.e. as long as  $d_1 > h$ ; within this range the films consist mainly of decoupled double layers, whereby the resistivity of one double layer (i.e. Ta–Cu and Ni–Cu, respectively) is larger than that of a ‘free’ double layer owing to the enhancement of the surface scattering of the upper half of this layer (i.e. the Cu part) by the lower component of the next double layer (i.e. Ta and Ni, respectively).

In order to investigate the breakdown of the multi-layered structure into a clustered structure Hall effect measurements have been carried out within the critical range of layer thicknesses.

#### 4.2. Hall effect

In multi-layered structures, it seems to be more convenient to give the results for the Hall voltage than those for the Hall coefficient; therefore we show in figures 2 and 3 the measured values of the Hall voltage for the Ta–Cu and Ni–Cu films, respectively. For Ta–Cu structures the theoretical curves are shown as a broken curve for the multi-layer model and as a full curve for the binary alloy model (equations (3) and (5), respectively). For the fitting calculations the following values have been used:  $R_{\text{H}}^{\text{Cu}} = -6.9 \times 10^{-11} \text{ m}^3 \text{ C}^{-1}$ ,  $\rho_{\infty}^{\text{Cu}} = 4.4 \mu\Omega \text{ cm}$ ,  $R_{\text{H}}^{\text{Ta}} = 10 \times 10^{-11} \text{ m}^3 \text{ C}^{-1}$ ,  $\rho_{\infty}^{\text{Ta}} = 205 \mu\Omega \text{ cm}$ ; the Hall

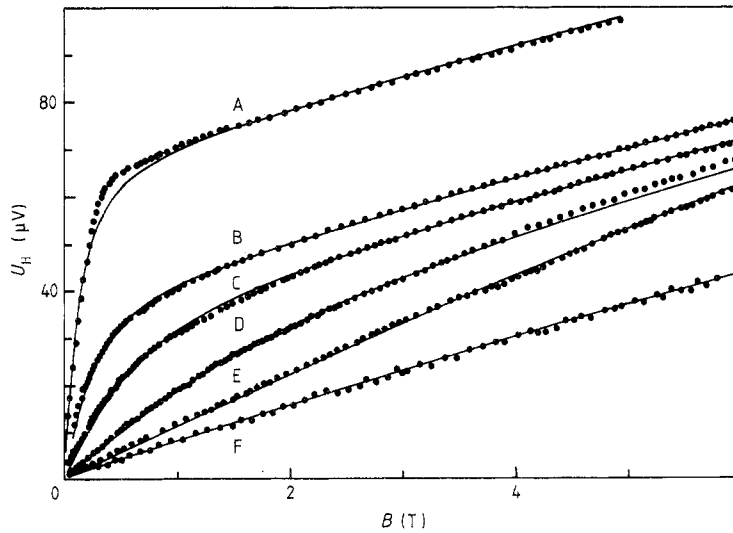


**Figure 3.** Hall voltage plotted against applied magnetic field for different layer thicknesses in Ni-Cu structures ( $I = 10$  mA;  $T = 300$  K; film width, 0.2 cm): ●, experimental results; —, Langevin function.  $d_1$  (in nm) is 2.65 (A), 1.8 (B), 1.55 (C), 1.25 (D), 0.8 (E), 0.4 (F).

coefficients correspond to experimental results from single-layer films of 25 nm thickness and the resistivities are taken from the foregoing discussion of the dependence of  $\rho$  on  $d_1$ . Note that it is not necessary to assume any thickness dependence of the Hall coefficients themselves (as predicted by the well known Sondheimer [17] theory) in order to fit the experimental data.

For large layer thicknesses, i.e. for  $d_1 > 5$  nm  $U_H$  is approximately constant and corresponds to the value for Cu, where the current density in the Cu layers is twice as large as the mean value due to the large resistivity of the Ta layers. Therefore the evaluation of the normal Hall constant  $R_H$  of the whole multi-layered film (in the following it is called the total Hall constant) by the simple formula  $R_H = U_H d / BI$ , where  $d$  is the total film thickness equal to approximately 100 nm and  $I$  is the total current, gives twice the value of the normal Hall constant of Cu within this range of layer thicknesses.

For smaller thicknesses the Hall voltage increases from negative values to zero and becomes positive for  $d_1 = 2$  nm. This is due to the positive values of the Hall coefficient of Ta and the increasing value for  $\rho_{Cu}(d_1)$  as given by equations (1) and (2); the current density within the Cu decreases, whereas it increases in Ta (note that Ta shows almost no size effect in  $\rho$  owing to its small MFP), leading to an increase in the total Hall constant from twice the negative Hall constant of Cu to positive values.

For all values of the layer thickness  $d_1$ , the dependence of the Hall voltage on  $d_1$  can be fitted without assuming a thickness dependence of the Hall coefficients of Ta and Cu, respectively; the 'size effect' shown by  $U_H$  against  $d_1$  is merely produced by the thickness-dependent resistivity of the Cu layers. Down to a thickness of about 2 nm the Hall voltage can be fitted very well by the model in [13] for multi-layered films (broken curve in figure 2); this indicates that within this range of layer thicknesses the films exhibit a continuous multi-layered structure, in which the current densities within each individual layer vary with the layer thickness owing to the size effect of the resistivity as discussed

above. For extremely small thicknesses ( $d_1 < 1.6$  nm) the measured Hall voltage deviates from the broken curve of the continuous-layer model in [13] and becomes closer to the model in [14] for binary alloys (full curve in figure 2). This behaviour again attests the breakdown of the multi-layered structure for the Ta–Cu films at the critical thickness  $d_1$  of 1.6 nm.

The measured absolute values of the Hall voltage for Ni–Cu structures are given in figure 3 as a function of the applied magnetic field  $B$  for different layer thicknesses (note that the total Hall coefficient defined above is negative for all values of  $d_1$  and  $B$  in the Cu–Ni system). For  $d_1 > 2$  nm a clear separation of the anomalous from the normal Hall voltage can be recognised. For magnetic fields below about 1 T, mainly the anomalous component of the Hall voltage produced by the Ni layers appears. Above 1 T, the magnetisation of the Ni component saturates; therefore, for  $B > 1$  T, the curve shows only the ordinary Hall voltage of the Ni–Cu multi-layers superimposed on the anomalous component due to the saturation magnetisation of Ni. For  $d_1 < 2$  nm the shape of the curves changes substantially. Even at the maximum available field of 6 T, no real saturation of the anomalous component can be observed, i.e. the magnetisation of the films is not constant even at these high applied fields. This effect can be attributed to an increasing tendency of the Ni component to form clusters with decreasing layer thickness. In this case a crossover from ferromagnetic to superparamagnetic behaviour should be observed. Therefore we fitted the theory (full curves) to the experimental data using equations (6) and (8) for the Hall effect and magnetisation, respectively. Again no thickness dependence of the Hall constants was assumed.

The normal component of the Hall voltage was calculated using the values of the normal Hall coefficients as measured for films 25 nm thick, i.e.  $R_H^{\text{Cu}} = -6.9 \times 10^{-11} \text{ m}^3 \text{ C}^{-1}$  and  $R_H^{\text{Ni}} = -6.0 \times 10^{-11} \text{ m}^3 \text{ C}^{-1}$ ; the extraordinary Hall constant of Ni was assumed to be  $R_{\text{He}}^{\text{Ni}} = -60 \times 10^{-11} \text{ m}^3 \text{ C}^{-1}$ . The results of this fitting procedure are shown as full curves in figure 3.

As mentioned above, the normal Hall coefficients for Ni and Cu are nearly equal; moreover the MFPS of the two materials are of the same order, too. Therefore, contrary to the Ta–Cu structure, the current density within one layer is nearly independent of  $d_1$  and consequently the normal component of the measured Hall voltage shows no variation with  $d_1$ .

On the contrary, the anomalous component of the Hall voltage, which is due to the Ni component only, shows apparently a strong thickness dependence. As discussed above, the magnetisation increases rapidly below  $B = 1$  T and shows complete saturation above  $B = 1$  T for layer thicknesses above 2 nm. Therefore the experimental results can hardly be reproduced by a Langevin function for  $d_1 > 2$  nm. Below 2 nm layer thickness, the experiment shows a much smoother increase in the magnetisation with increasing applied field; within this range of layer thicknesses, the curves therefore can be fitted very well by equation (8) (Langevin function) together with the usual normal component of the Hall voltage, indicating the dominant role of superparamagnetism of small non-interacting Ni clusters in these films.

Using the value of  $\mu$  for the mean magnetic moment of one Ni cluster resulting from the fitting calculations described above, the mean number of Ni atoms per cluster is estimated using equation (7) with an assumed magnetic moment of  $0.6 \mu_B$  per Ni atom (bulk value); additionally the size of the Ni clusters can be roughly estimated using the mean number of atoms per cluster and the next-nearest-neighbour distance of 0.25 nm.

From the volume of one Ni cluster the mean base plane occupied by all clusters can be evaluated if the shape of the clusters is assumed to be hemispherical which is very

**Table 2.** Results from fitting the Langevin function to the measured dependence of  $U_H$  on the applied magnetic field.

Layer thickness $d_1$ (nm)	Number $n$ of Ni atoms per cluster	Radius $R$ of one cluster (nm)	Ratio $r$ of cluster base plane to film area
0.4	140	0.57	0.52
0.8	240	0.74	0.85
1.25	940	1.10	0.85
1.55	2400	1.15	0.8
1.8	2600	1.5	0.9
2.65	7700	2.2	0.95

likely in layered materials. The dimensionless value  $r$  introduced in table 2 is the ratio of this base plane of all Ni clusters within one layer to the total film area. Clearly the critical value of this ratio is close to unity. For  $r < 1$ , the base plane of all Ni clusters is smaller than the film area and therefore well separated Ni particles should exist in this case. If  $r$  reaches unity, the Ni clusters should percolate and a crossover from superparamagnetic ( $r < 1$ ) to pure ferromagnetic behaviour ( $r > 1$ ) can be expected. The results of these calculations are given in table 2. The number of Ni atoms per cluster increases with increasing layer thickness. The value  $r$  introduced above is substantially smaller than unity for  $d_1$  below 1.8 nm and approaches unity above this layer thickness, indicating again a crossover from a clustered to a multi-layered film structure at this critical thickness.

Although the approach given above seems to be somewhat crude (the accuracy is 20% for the number of atoms per cluster and 10% for the radius), good agreement between the evidences of the  $\rho$  against  $d_1$  and the  $U_H$  against  $d_1$  dependence can be stated for Ni–Cu. Above a layer thickness of 1.5 nm the films are multi-layered, showing a well known size correction in the resistivity and ferromagnetism in the anomalous Hall voltage. Below 1.5 nm the resistivity saturates to the value of Ni–Cu alloys; the Hall voltage indicates a breakdown from the ferromagnetism of continuous multi-layers to a clustered structure with superparamagnetic behaviour of well separated Ni particles. For all values of the layer thickness the sign of both the normal and the extraordinary Hall constant is negative. The dependence of the Hall voltage on  $d_1$  and on the applied magnetic field  $B$  can again be fitted without assuming any thickness dependence of both types of Hall constant. The variation in the normal component of the Hall voltage with  $d_1$  is negligible for the Cu–Ni films (in contrast with the Ta–Cu system), because the individual layer resistivities of the Ni and Cu layers depend in nearly the same way on the layer thickness. The variation in the anomalous component of  $U_H$  with  $d_1$  for  $d_1 < 2$  nm is caused by the smooth crossover from ferromagnetic to superparamagnetic behaviour for this range of layer thickness. Direct measurements of the magnetisation of the Ni–Cu multi-layered structures will be presented elsewhere [18].

## 5. Conclusions

In the present paper, investigations of resistivity and Hall effect in multi-layered Ta–Cu and Ni–Cu thin films have been presented. Both types of material show a well defined

multi-layered structure down to layer thicknesses of about 1.5 nm. Within this range of continuous films, both the resistivity and the Hall voltage can be described by a simple model of parallel switched double layers, in which the resistivity shows an increase with decreasing layer thickness owing to enhanced, completely diffuse interface scattering of the conduction electrons. This size effect can be very well described by the usual single-layer Fuchs–Namba theory [7, 10].

In contrast with the resistivity the Hall coefficients do not show any kind of thickness dependence. The apparent dependence of the measured Hall voltage on the layer thickness can be simply explained by taking into account the thickness-dependent current densities in the layers caused only by the variation in the single-layer resistivity with the layer thickness  $d_1$ . For thicknesses above 2 nm the anomalous Hall effect observed in Ni–Cu films is typical for ferromagnetic behaviour of the Ni component.

Below this critical thickness, both the resistivity and the Hall effect for both types of film give evidence of a breakdown of the multi-layered structure to a clustered island-like structure. As expected by the theoretical models discussed in § 1, the resistivity saturates close to the values of the corresponding alloys. The Hall voltage for Ta–Cu changes its sign owing to the large positive Hall coefficient of Ta and saturates at a value predicted by a model dealing with binary alloys. For Ni–Cu films the dependence of the anomalous Hall voltage on the applied field changes substantially at this critical thickness from typical ferromagnetic to superparamagnetic behaviour which can be quantitatively described by a Langevin function. There seems to be no need to assume the appearance of a ‘dead magnetic layer’ of Ni in order to explain the experimental data; this effect can be simply understood as a crossover from a multi-layered to a clustered film structure at the critical values of the layer thickness.

## References

- [1] Bezak V, Kedro M and Pevala A 1974 *Thin Solid Films* **23** 305
- [2] Carcia P F and Suna A 1983 *J. Appl. Phys.* **54** 2000
- [3] Dimmich R 1985 *J. Phys. F: Met. Phys.* **15** 2477
- [4] Gurvitch M 1986 *Phys. Rev. B* **34** 540
- [5] Chen Chu-Xing 1986 *Appl. Phys. A* **40** 37
- [6] Chen Chu-Xing 1987 *Appl. Phys. A* **42** 145
- [7] Fuchs K 1938 *Proc. Camb. Phil. Soc.* **34** 100
- [8] Hoffmann H, Vancea J and Jacob U 1985 *Thin Solid Films* **129** 181
- [9] Hoffmann H, Hornauer H, Jacob U and Vancea J 1985 *Thin Solid Films* **131** 1
- [10] Sondheimer E H 1952 *Adv. Phys.* **1** 1
- [11] Namba Y 1970 *Japan. J. Appl. Phys.* **9** 1326
- [12] Vancea J, Hoffmann H and Kastner K 1984 *Thin Solid Films* **12** 201
- [13] Petritz R L 1958 *Phys. Rev. B* **6** 1254
- [14] Adkins C J 1973 *J. Phys. C: Solid State Phys.* **12** 3389
- [15] Hurd C M 1972 *The Hall Effect in Metals and Alloys* (New York: Plenum)
- [16] Ashcroft N W and Mermin N D 1976 *Solid State Physics* (New York: Holt, Rinehart and Winston)
- [17] Sondheimer E H 1950 *Phys. Rev.* **80** 401
- [18] Robl W 1987 *Diploma Thesis* University of Regensburg